Tribological behaviour of copper oxide nanoparticle suspension

J.E. Fernández[1], J.L. Viesca[1,*], A. Hernández Battez[1]

University of Oviedo
[1] Department of Mechanical and Civil Engineering. Ctra. de Castiello s/n. 33204 Gijon. Spain.
[*] Phone: 34-985103000 ext. 5849 Fax: 34-985182433 Email: viescajose@uniovi.es

ABSTRACT

This work presents and discusses the tribological behaviour of nanoparticle suspensions in a polyalphaolefin (PAO6). CuO nanoparticles were separately dispersed at 0.5, 1.0 and 2.0% wt. in PAO6 using an ultrasonic probe for 2 minutes. AW properties were obtained using a TE53SLIM tribometer with a block-on-ring configuration and EP properties were obtained using a Four-Ball machine according to ASTM D2783. Wear surfaces were analyzed by SEM and EDS after tests. The study led to the following conclusions: nanoparticle suspensions exhibited reductions in friction and wear compared to the base oil; CuO suspensions showed the highest friction coefficient and lowest wear per nanoparticle content of 2%; all concentrations of nanoparticles improved the EP properties of PAO6; CuO showed better results at 0.5% wt. of nanoparticles; and the antiwear mechanism of nanoparticulate additive was produced by tribo-sintering.

Keywords: nanoparticles, CuO, additives, wear behaviour, lubricant.

1. INTRODUCTION

Friction and surface damage caused by high temperatures and pressures can be reduced by applying extreme pressure (EP) and antiwear (AW) additives. These tend to be sulphur-, chlorine-, and phosphorous- containing compounds designed to react chemically with the metal surfaces, forming easily sheared layers of sulphides, chlorines, or phosphides, and thereby preventing severe wear and seizure [1].

The application of inorganic nanoparticles has been the focus of particular research attention for some 25 years. The tribological properties of LaF_3 [2], graphite [3], polytetrafluoroethylene (PTFE) [4], MoS_2 [5], TiO_2 [6-8], $La(OH)_3$ [9], PbS [10], lanthanum borate [11], titanium borate [12], zinc borate [13], ferric oxide [14], ferrous borate [15], Ni [16], $CaCO_3$ [17] and ZnO [18] nanoparticles used as oil additives have all been investigated in that time. Results show that they can deposit on the rubbing surface and improve the tribological properties of the base oil. Micron particles of a certain hardness have also been reported to lead to abrasive friction [19]. The results observed by Xue et al. [8] and Dong et al. [17] also point to nanoparticles displaying good friction and wear reduction characteristics even at concentrations below 2%wt.

Copper oxide nanoparticles with a diameter of 10-40 nm have also been tested recently as an additive in cutting fluids [20]. Transfer and adhesion of the micellar particles accelerated surface modification, self-reducing and forming of a fine copper tribofilm that reduced the coefficient of friction, the extent of direct contact between the cutting tool and the workpiece, the temperature in the cutting zone and hence tool wear.

This paper studies the antiwear behaviour of CuO nanoparticle suspensions in a polyalphaolefin (PAO6) under mixed lubrication using a block-on-ring tribometer and uses a four-ball machine to study the extreme-pressure behaviour also. SEM and EDS was used to analyse wear scar surfaces. Taking into account the results obtained by Pawlak [20] and Cambiella [21], some of the potential applications of these nanoparticles as additives in a polyalphaolefin can be found in metalworking fluids and also in lubricants for gearboxes.

2. EXPERIMENTAL DETAILS

2.1 Nanoparticles and lubricant

The main properties of the nanoparticles and lubricant are listed in Table 1. CuO nanoparticles were separately dispersed in the lubricant in concentrations of 0.5-1.0-2.0%wt. using an ultrasonic probe for 2 minutes.

Table 1 Material properties.

Materials	*Properties*					
Nanoparticles	*Morphology*	*Purity* (%)	*Size* (nm)	*Melting Point (°C)*	*Crystal System*	*Hardness (Mohs)*
CuO	Nearly spherical	99.0	30-50	1326	monoclinic	3.5
Base oil	*Physical properties*					
PAO6	Density (15.6°C): 0.826 g/cm^3 Viscosity: 31.0 cSt (40°C) 5.90 cSt (100°C) VI: 135					
Specimens	*Chemical composition*					
Block – AISI 1045	0.40-0.50%C, 0.15-0.40%Si, 0.50-0.80%Mn, <0.035%P, <0.035%S					
Ring – AISI D3	1.90-2.20%C, 0.10-0.60%Si, 0.20-0.60%Mn, 11.0-13.0%Cr, <0.03%P, <0.03%S					
Ball – AISI 52100	0.98-1.1%C, 0.15-0.30%Si, 0.25-0.45%Mn, 1.30-1.60%Cr, <0.025%P, <0.025%S					

2.2. Antiwear test procedure

All test-section components were cleaned ultrasonically with heptane for 3 minutes, rinsed in ethanol and dried with hot air before and after tests. Wear testing was undertaken using a TE53SLIM friction and wear testing machine set for pure sliding contact, with a block-on-ring configuration. Test blocks of 12.7 mm AISI 1045 steel cubes with a hardness of about 31 HRC were run against a 60 mm-diameter AISI D3 steel counterface ring, hardened in the range 65-66 HRC. All tests were run for a total distance of 3066 m. at a sliding speed of 2 m/s and a load of 165 N applied via a cantilever. Two tests were conducted for each suspension at this load, and wear was quantified by weight loss (± 0.1 mg). The friction coefficient was recorded throughout each test by means of a load transducer positioned to measure the lateral force on the block specimen. Wear surfaces on blocks were characterised using scanning electron microscopy (SEM) and energy dispersive spectrometry (EDS) was used to detect the elements present on the blocks.

2.3 Extreme pressure test machine and procedure

All test-section components were cleaned ultrasonically with heptane for 3 minutes, rinsed in ethanol and dried with hot air before and after tests. The test machine used for extreme pressure tests (ASTM D2783) was a Four-Ball machine with a drive shaft speed of 1470 rpm. The 12.7 mm diameter test balls with a roughness of R_a = 0.035 μm used in this study were made from AISI 52100 steel with a hardness of 65 RC (Table 1). In this technique, one steel ball under load is rotated against three steel balls held stationary in the form of a cradle while immersed in the lubricant. A series of 10 tests of 10-second duration are carried out at increasing loads until welding occurred, Fig. 1. The first run was made at an initial load of 490 N and the additional runs were carried out at consecutively higher loads according to the standard method: 617, 980, 1235, 1568, 1960, 2450, 3087 N… until welding occurs. If ten loads have not been run when welding occurs, the total was brought to ten by assuming,

according to the standard, that loads below the last nonseizure load produce wear scars equal to the compensation scar diameter. The wear scar diameters (WSD) in the stationary balls were measured using a Nikon PFX optical microscope, provided with a Nikon F-301 CCD camera, and plotted against the applied load. From the EP results, the following parameters were obtained: initial seizure load (ISL), weld load (WL) and load-wear index (LWI). Repeatability and reproducibility were verified according to ASTM D2783 recommendations.

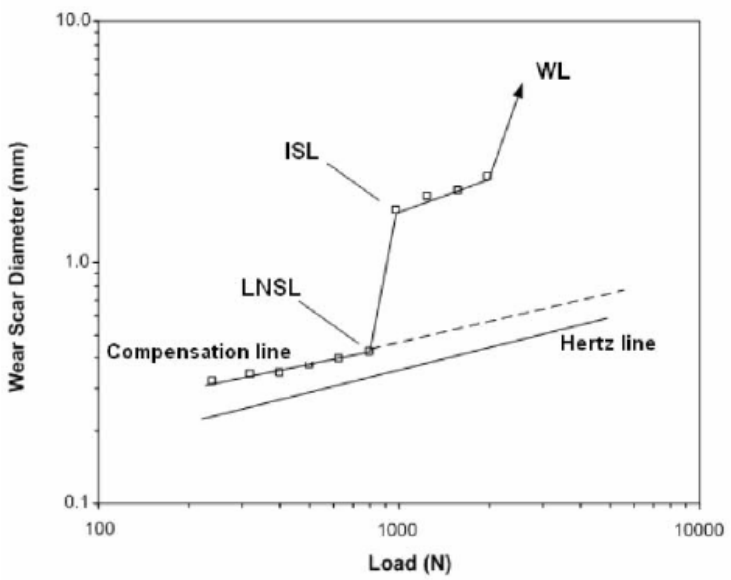

Figure 1. Example of a wear-load curve obtained from the extreme pressure tests.

2.2.1 Hertz line

The Hertz line was obtained by plotting the Hertz scar diameter against the load. The Hertz scar diameter (d_h) is the average diameter of an indentation caused by the deformation of the balls under static conditions.

2.2.2 Compensation line

The compensation line was obtained from a plot of the compensation scar diameters against the applied load. The compensation scar diameter is the average diameter of the wear scar on the stationary balls, caused by the rotating ball under an applied load in the presence of lubricant, but without causing either seizure or welding.

2.2.3 Last nonseizure load (LNSL), initial seizure load (ISL) and weld load (WL)

The last nonseizure load (LNSL) is the last load at which the measured scar diameter is not higher than 5% above the compensation line. Usually, the region beyond the LNSL is known as *extreme pressure (EP) region*, whereas the region before the LNSL is the *antiwear (AW) region*. According to employed loads, we define initial seizure load (ISL) as the first load beyond the LNSL. The weld load (WL) is the lowest applied load at which the rotating ball welds to the three stationary balls.

2.2.4 Load-wear index (LWI)

The load wear index (LWI) is a single parameter (the higher the better) that shows the overall EP behaviour in a range between well below seizure and welding. It may be calculated from the expression:

$$LWI = \frac{\sum_{i=1}^{n} \frac{P_i \, d_{h,i}}{d_i}}{n} \qquad (1)$$

where P is the applied load, d_h the Hertz diameter, d the wear scar diameter and n the total number of occurrences.

2.3 Worn surface analysis

The topography of the wear scar surface was studied by scanning electron microscopy (SEM JEOL-6100); energy dispersive spectrometry (EDS) was used to detect the elements present on wear scar surfaces.

3. RESULTS AND DISCUSSION

3.1 Antiwear tests

Fig. 2 illustrates how all nanoparticle concentrations in PAO6 diminished the friction coefficient compared to pure PAO6. However, results for each suspension differed depending on nanoparticle concentration. The lowest friction coefficient was obtained at 1% and the highest at 2% of CuO. The highest friction coefficient and lowest friction reduction was provided by the PAO 6 + 2%CuO suspension, Fig. 3. In contrast this mixture also exhibited the lowest wear, with a reduction of about 60% in comparison with pure PAO 6.

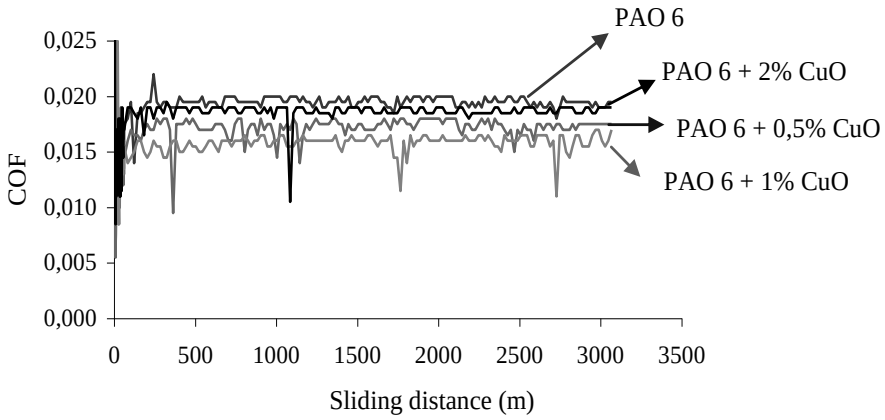

Figure 2. Friction as a function of sliding distance for PAO 6 + CuO suspensions.

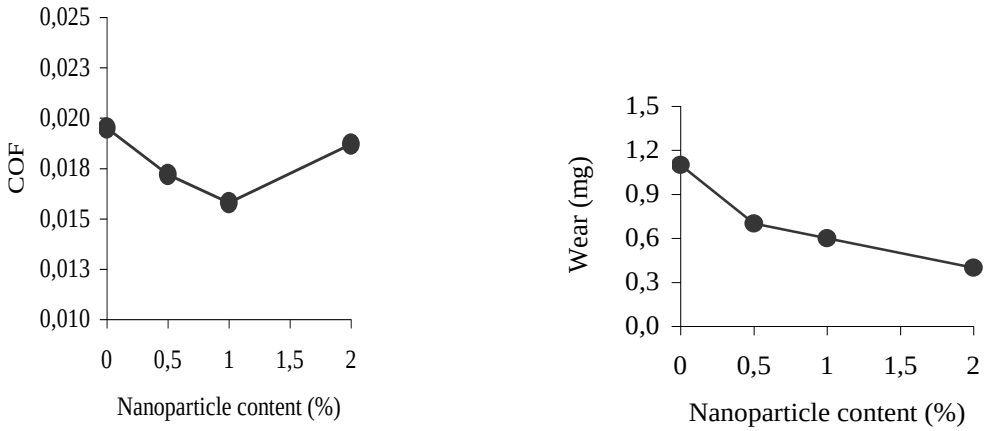

Figure 3. Friction coefficient and wear as a function of nanoparticle concentration for all tested suspensions.

Friction and wear variations of suspensions as a function of nanoparticles content are related to size, hardness and deposition of nanoparticles on wear surfaces. Friction coefficient values in all tests are for a mixed lubrication regime in which lubricant film thicknesses are between 3 and 25 nm [22]. According to Chiñas and Spikes' mechanical entrapment theory [23], nanoparticles penetrate in the

contact area and then deposit on it because they are smaller or similar in size to lubricant film thickness. On the other hand, nanoparticles have a deleterious effect in some cases, increasing either friction or wear [24].

No chemical elements other than steel components were detected on the wear surface obtained after tests made with pure PAO 6. Although CuO have lower bulk hardness than steel, greater displacement of materials across the wear surface is observed in the case of the PAO6 + 2%CuO suspension. This behaviour could be related to CuO being larger than lubricant film thickness in mixed regimen and therefore being more likely to be trapped (percentage deposited: 0.53) and flattened at the contact area, offering a much larger interface for friction. The nanoparticle hardness cited is the bulk hardness, but due to the well-established Hall–Petch relationship (abbreviated as H-P relation) the hardness of all used nanoparticles is higher than the specimens´ hardness, even taking into account the inverse H-P relation [25-26]. This can explain the abrasive behaviour found in some cases.

More analysis of the wear surfaces was done in order to detect a possible tribofilm formation. Although copper was detected, agglomeration or a uniform deposition of nanoparticles were not found on the wear surfaces, Fig. 4.

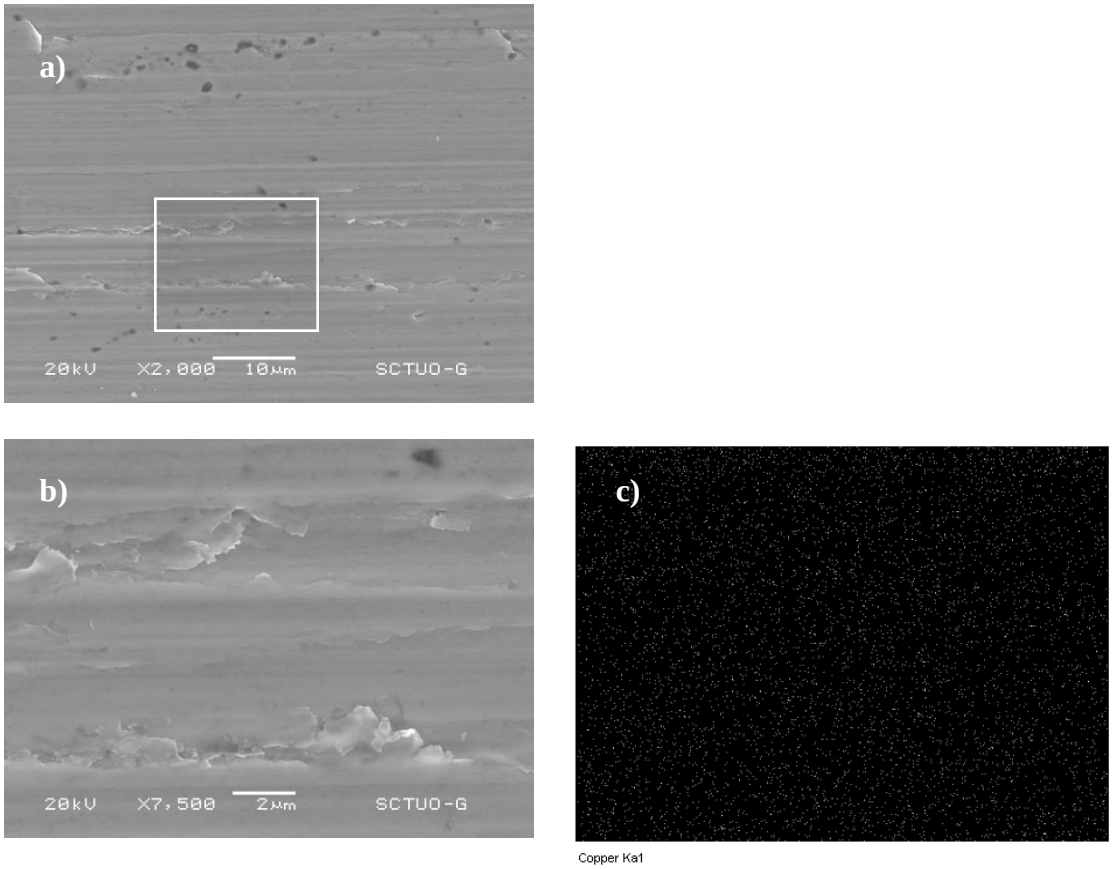

Figure 4. SEM micrographs and mapping of the wear surface for the PAO6 + 2%CuO suspension: b) is a high-magnification micrograph of the marked area of a), and c) is the mapping of b).

The antiwear mechanism of nanoparticulate additive can follow three different processes: the nanoparticles may be melted and welded on the shearing surface (this option is impossible for the nanoparticles here studied because their melting point is 1326ºC), reacted with the specimen to form a protective layer (this option is unlikely due to electropositive nature of metal oxide nanoparticles and specimens´ material), or tribo-sintered on the surface [21]. This last option is the most likely one here and was also verified by Kato et al. [27] using nanometer-sized oxide nanoparticles as solid lubricant. In addition, Zhou et al. [28] showed that, when very fine metallic particles are employed, sintering starts as soon as the temperature increases above room temperature.

3.2 Extreme pressure tests

Figure 5 illustrates how all nanoparticle concentrations in PAO6 diminished the wear scar diameter from initial seizure load onwards. As a result, the load wear index (LWI) increased with the addition of all three nanoparticles to PAO6. PAO6 + CuO suspensions had better results when the nanoparticle concentrations were of 0.5% and 2%, as shown in Table 2. Although the LWI was improved in all cases compared to PAO6, the initial seizure load and weld load maintained the same values as for PAO6. In contrast and interestingly, the WSD for each suspension at ISL is significantly different from PAO6.

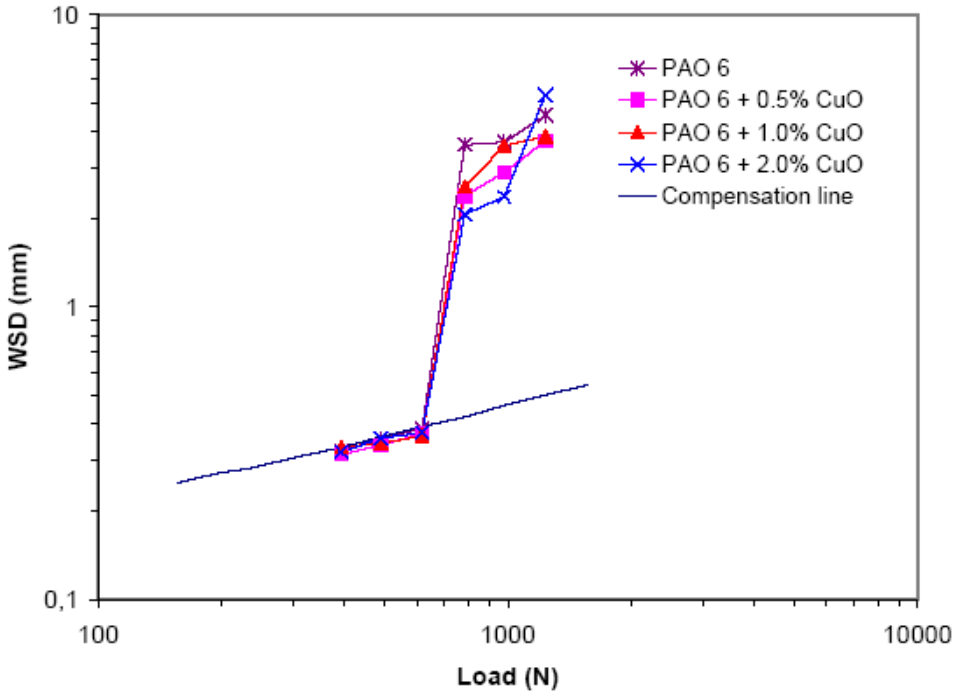

Figure 5. Log load versus log wear scar diameter of PAO6 + CuO suspensions.

Table 2. Extreme pressure properties of tested suspensions.

Lubricant	*Initial seizure load, ISL (N)*	*Mean wear scar diameter at ISL (mm)*	*Weld load, WL (N)*	*Load Wear Index, LWI (N)*
A	784.8	3.584	1569.6	248.19
B	784.8	2.402	1569.6	263.29
C	784.8	2.578	1569.6	257.78
D	784.8	2.073	1569.6	260.39

A: PAO6
B: PAO6 + 0.5% CuO
C: PAO6 + 1.0% CuO
D: PAO6 + 2.0% CuO

The above results refer to nanoparticle behaviour at the contact point. Wear behaviour of suspensions are identical to pure PAO6 below the ISL (Fig. 5), and no nanoparticle deposition was found on the wear scar. These results seem to be related to the short test time and that tests are performed in the AW region. In contrast, different results can be seen at ISL. Nanoparticle deposition behaviour in the PAO6 + CuO suspensions at ISL, Fig. 6, was of 0.51 and 2.20% for the suspensions with 0.5 and 2% of CuO, respectively. Although there was an appreciable decrease of WSD at ISL for PAO6 + 2%CuO compared to PAO6 + 0.5%CuO.

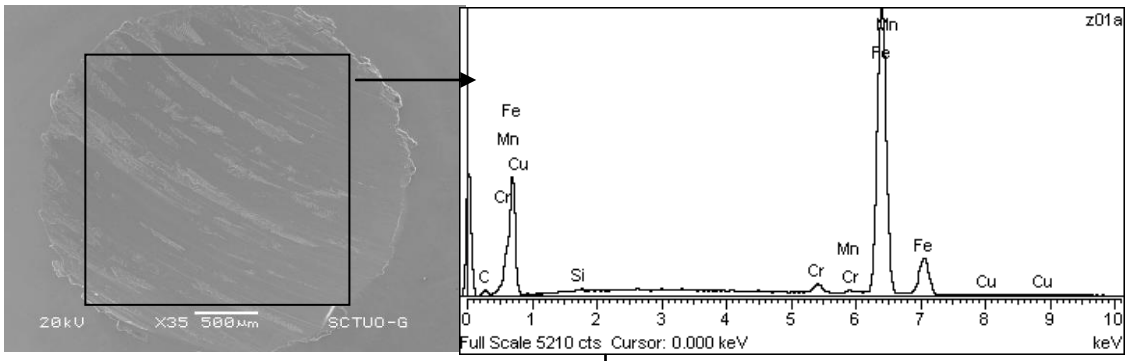

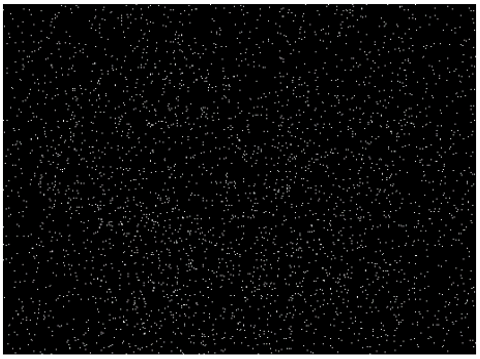

Element	Weight%	Atomic%
C K	3.76	15.34
Si K	0.23	0.40
Cr K	1.43	1.35
Mn K	0.41	0.36
Fe K	93.66	82.15
Cu K	0.51	0.39

(a)

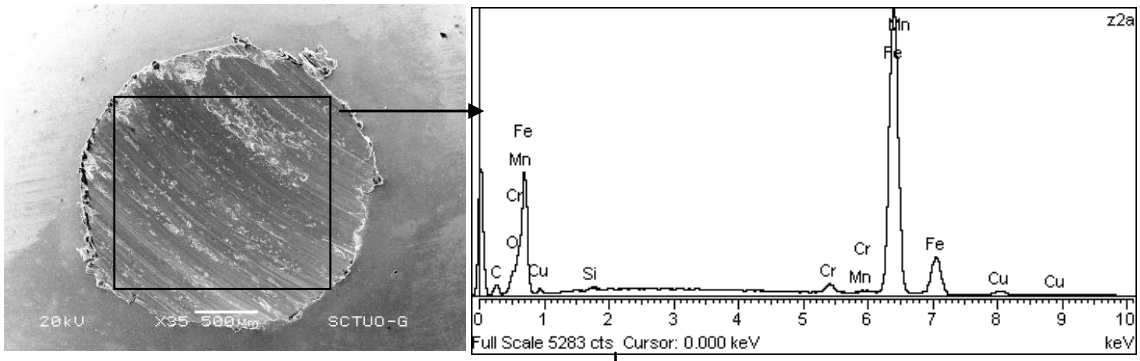

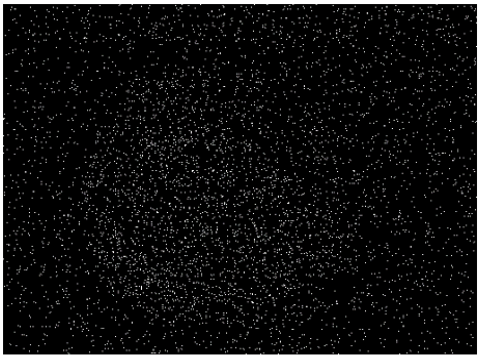

Element	Weight%	Atomic%
C K	6.64	22.84
Si K	0.28	0.42
Cr K	1.44	1.14
Mn K	0.28	0.21
Fe K	84.81	62.74
Cu K	2.20	1.43

(b)

Figure 6. Micrograph, elemental analysis, and mapping at initial seizure load of:
(a) PAO6 + 0.5%CuO, (b) PAO6 + 2.0%CuO

The antiwear mechanism of nanoparticulate additive can be explained as follows. When the lubricant film between tribo-pairs becomes thinner and mixed lubrication or boundary lubrication occurs (from LNSL onward), the nanoparticles may carry a proportion of load and separate the two surfaces to prevent adhesion, thus benefit the antiwear properties. All aspects with regard size, hardness and deposition mechanisms explained in section 3.1 are applicable here too.

4. CONCLUSIONS

The following conclusions can be drawn from the results presented above:

- All nanoparticle suspensions exhibited friction and wear reduction compared to the base oil. However, the suspension with 2% of CuO had the highest friction coefficient and lowest wear.
- An increase of nanoparticle concentration in base oil increases deposition on wear surfaces. Nevertheless, tribological results can differ with regard to friction and wear.
- All nanoparticle suspensions improve the EP properties of PAO6. However, the PAO6 + 2%CuO suspensions exhibited the best EP behaviour, with a higher LWI than pure PAO6 and the lowest WSD at ISL.
- The AW and EP results of tested suspensions were related to the size, hardness, and deposition mechanisms of the nanoparticles.

ACKNOWLEDGMENT

The authors wish to express their thanks to the Ministry of Education and Science, Spain, for supporting this work within the framework of the Research Project MAT2003-06153.

REFERENCES

[1] W. Huang, Y. Tan, J. Dong, B. Chen, Tribological properties of the film formed by borated dioctyl dithiocarbamate as an additive in liquid paraffin, Tribology International 35 (2002) 787-791.
[2] J. Zhou et al., Study on an antiwear and extreme pressure additive of surface coated LaF_3 nanoparticles in liquid paraffin, Wear 249 (2001) 333-337.
[3] T. Hisakado, T. Tsukizoe, H. Yoshikawa, Lubrication Mechanism of Solid Lubricants in Oils, ASME J. Lubr. Technol. 105 (1983) 245–253.
[4] F.G. Reick, Energy Saving Lubricants Containing Colloidal PTFE, Lubr. Eng. 38 (1982) 635–646.
[5] J. Gansheimer, R. Holinski, Molybdenum Disulfide in Oils and Greases under Boundary Conditions, ASME J. Lubr. Technol. 95 (1973) 242–248.
[6] Z.S. Hu, J.X. Dong, Study on antiwear and reducing friction additive of nanometer titanium oxide, Wear 216 (1998) 92–96.
[7] Y. Gao et al., Study on tribological properties of oleic acid-modified TiO_2 nanoparticle in water, Wear 252 (2002) 454-458.
[8] Q. Xue, W. Liu, Z. Zhang, Friction and wear properties of a surface modified TiO_2 nanoparticle as an additive in liquid paraffin, Wear 213 (1997) 29-32.
[9] Z. Zhang, W. Liu, Q. Xue, Study on lubricating mechanisms of $La(OH)_3$ nanocluster modified by compound containing nitrogen in liquid paraffin, Wear 218 (1998) 139–144.
[10] S. Chen, W. Liu, L. Yu, Preparation of DDP-coated PbS nanoparticles and investigation of the antiwear ability of the prepared nanoparticles as additive in liquid paraffin, Wear 218 (1998) 153–158.
[11] Z.S. Hu, J.X. Dong, G.X. Chen, J.Z. He, Preparation and tribological properties of nanoparticle lanthanum borate, Wear 243 (2000) 43-47.
[12] Z.S. Hu, J.X. Dong, Study on antiwear and reducing friction additive of nanometer titanium borate ,Wear 216 (1998) 87-91.
[13] J.X. Dong, Z.S. Hu, A study of the anti-wear and friction-reducing properties of the lubricant additive, nanometer zinc borate, Tribology International 31 (1998) 219-223.
[14] Z.S. Hu, J.X. Dong, G.X. Chen, Study on antiwear and reducing friction additive of nanometer ferric oxide, Tribology International 31 (1998) 355-360.
[15] Z.S. Hu, J.X. Dong, G.X. Chen, Preparation and tribological properties of nanometer SnO and ferrous borate as lubricant additives, 98' Asia International Tribology Symposium, Pekin, China (1998) .
[16] S. Qiu, Z. Zhou, J. Dong, G. Chen, Preparation of Ni nanoparticles and evaluation of their tribological performance as potential additives in oils, J. of Tribology 123 (2001) 441-443.
[17] J.X. Dong, G. Chen, S. Qiu, Wear and friction behaviour of $CaCO_3$ nanoparticles used as additives in lubricating oils, Lubr. Sci. 12 (2000) 205-212.
[18] A. Hernandez Battez, et al., The tribological behaviour of ZnO nanoparticles as an additive to PAO6, Wear 261 (2006) 256-263.
[19] J.K. Knapp, H. Nitta, Fine-particle slurry wear resistance of selected tungsten carbide thermal spray coatings, Trib. Int. 30 (1997) 225–234.
[20] Z. Pawlak, et al., The tribochemical and micellar aspects of cutting fluids, Trib. Int. 38 (2005) 1–4.

[21] A. Cambiella, et al., Formulation of emulsifiable cutting fluids and extreme pressure behaviour, J. Mater. Process Tech. 184 (2007) 139–145.
[22] B. Bhushan, Principles and Applications of Tribology, Wiley-Interscience, 1999, 1020 p.
[23] F. Chiñas-Castillo, H.A. Spikes, Mechanism of action of colloidal solid dispersions, J. of Tribology, Trans. ASME 125 (2003) 552–557.
[24] H. Mishina, et al., Lubricity of the metallic ultrafine particles, Jpn. J. Tribol. 38 (1993) 1109-1120.
[25] Y.B. Pithawalla et al., Preparation of ultrafine and nanocrystalline FeAl powders, Materials Science and Engineering A329–331 (2002) 92–98.
[26] S. Takeuchi, The mechanism of the inverse Hall-Petch relation of nanocrystals, Scripta mater. 44 (2001) 1483–1487.
[27] H. Kato, K. Komai, Tribofilm formation and mild wear by tribo-sintering of nanometer-sized oxide particles on rubbing steel surfaces, Wear 262 (2007) 36-41.
[28] Y.H. Zhou, M. Harmelin, J. Bigot, Sintering behavior of ultra-fine Fe, Ni, and Fe–25 wt.%Ni powders, Script. Metall. 23 (1989) 1391–1396.